Frontiers of Information Technology & Electronic Engineering
www.jzus.zju.edu.cn; engineering.cae.cn; www.springerlink.com
ISSN 2095-9184 (print); ISSN 2095-9230 (online)
E-mail: jzus@zju.edu.cn

Correspondence:

Zero ground clearance dual antenna pair for metal-cased fifth-generation multiple input multiple output smartphone*

Le CHANG†‡[1], Wenbao HE[1], Xiaomin CHEN[2], Xiaoxue TAN[1], Juan CHEN[1], Kai KANG[3], Yang YANG[4]

[1]*School of Information and Communications Engineering, Xi'an Jiaotong University, Xi'an 710049, China*

[2]*School of Electronic Information Engineering, Inner Mongolia University, Hohhot 010021, China*

[3]*Department of the Europe and Asia, China Electronics Industry Engineering Co., Ltd., Beijing 100846, China*

[4]*Department of the Government and Enterprise, China Justice Big Data Institute, Beijing 100043, China*

†E-mail: changle4015@126.com

Received Mar. 27, 2022; Revision accepted June 21, 2022; Crosschecked July 20, 2022; Published online Aug. 12, 2022

https://doi.org/10.1631/FITEE.2200119

1 Introduction

The fifth-generation (5G) era has already arrived and many applications are prospering. The multiple input multiple output (MIMO) system is the key to enhancing channel capacity for both the fourth-generation (4G) wireless communication and 5G systems. For a smartphone, the most challenging task for antenna engineers is to accommodate the numerous 4G and 5G multi-port antennas while avoiding mutual coupling problems (Li Y et al., 2009, 2012; Hong, 2017; Sharawi et al., 2017). Therefore, implementing multiple antennas within a small space is a worthwhile topic to study, especially for antennas operating at the same frequency.

Recently, several studies have reported how to accommodate two co-frequency antennas with good mutual coupling performance within the same area (Li MY et al., 2017a, 2017b; Wong et al., 2017a, 2017b, 2017c; Sun et al., 2018; Chang et al., 2019, 2020, 2021). An orthogonal polarization method and a proper antenna layout selection can help mitigate the mutual coupling problem (Li Y et al., 2010b, 2011; Chen et al., 2019). Orthogonal modes are excited in the same radiator including a one-wavelength loop and quarter-wave open cavity, and an in-phase loop and slot (Li MY et al., 2017a, 2017b; Sun et al., 2018), whereas two orthogonal radiators including a T-shaped monopole and a floating dipole are excited separately within the same area (Chang et al., 2019). In Wong et al. (2017a, 2017b, 2017c), although the two kinds of antennas in an antenna pair are both identical in-phase current antennas/inverted F antennas, a coupled feed method and proper antenna layout solve the coupling problem.

Full screen has become an indispensable slogan for all manufacturers' flagship products (Han et al., 2019; Huang et al., 2019). Small ground clearance is one of the preconditions for full screen smartphones. For a modern smartphone, the ground clearance is less than 2 mm (Wong et al., 2017a, 2017b, 2017c; Sun et al., 2018; Chang et al., 2019, 2021; Deng et al., 2019). Moreover, considering the esthetic appearance

‡ Corresponding author

* Project supported by the National Natural Science Foundation of China (No. 62101427), the Key Research and Development Project of Shaanxi Province, China (No. 2022GY-095), the High-Level Innovation Talent Project Imported by Qinchuangyuan of Shaanxi Province, China (No. QCYRCXM-2022-33), and the Shaanxi Key Laboratory of Deep Space Exploration Intelligent Information Technology (No. 2021SYS-04)

ORCID: Le CHANG, https://orcid.org/0000-0002-4641-5792

and mechanical robustness, a metal-cased smartphone or one with an all-metal identity, such as a smartphone with metallic bezels and back cover, is another fashion trend (Wong and Tsai, 2016, 2017). However, a metallic back cover can deteriorate impedance matching and reduce radiation efficiency for antennas deployed in ground clearance. Therefore, antennas without ground clearance are important to achieve high performance in metal-cased smartphones. It is important to distinguish between the proposed antenna and the one proposed by Chang et al. (2019). Although these two antennas share the same radiating principle, our proposed implementation style prevents the antenna from being the obstacle to creating a full-screen and metal-cased smartphone, which is especially useful for realistic engineering.

A dual antenna pair working in the same frequency with zero ground clearance has been proposed for the first time. The proposed antenna pair is a simple T-shaped slot on the metallic bezel. Two orthogonal polarization characteristic modes including the in-phase current mode and the slot mode are excited simultaneously in the same antenna structure. Simulation results from using the proposed dual antenna pair show good impedance matching, isolation better than 24.5 dB, an envelope correlation coefficient (ECC) of less than 0.01, and total efficiency ranges of 50.3%–55.2% and 50.1%–63.1%. To verify the feasibility, the proposed four-antenna MIMO system is fabricated and tested. The measurement results are consistent with the simulation ones.

2 Operation principle

The operation principle and operating modes of the proposed antenna are illustrated in Fig. 1. Fig. 1a shows a metal-cased phone model consisting of a complete metallic back cover and four enclosed metallic bezels. The back cover is located at the bottom opening plane of the cavity formed by the four bezels. The proposed dual antenna pair is actually a combination of a rectangular slot and a split. Importantly, no ground clearance is needed.

The two characteristic modes of the proposed structure are illustrated in Fig. 1b. For mode 1, a 180° phase difference exists between the two sides of the split, and the E-fields are built across the split. A quarter-wave field is distributed on each open slot and the two open slots have reversed phases. The current flows around the slot in the same direction, either clockwise or counter-clockwise. This in-phase current excites the ground current in the *Y* direction, producing *Y*-polarized radiation. Mode 2 is a typical slot mode. Unlike mode 1, there is no potential difference across the split, so the E-fields on the slot have the same phase and orientation, producing *X*-polarized radiation. Therefore, these two orthogonal modes make it feasible to design a dual antenna pair with a high irrelevance property.

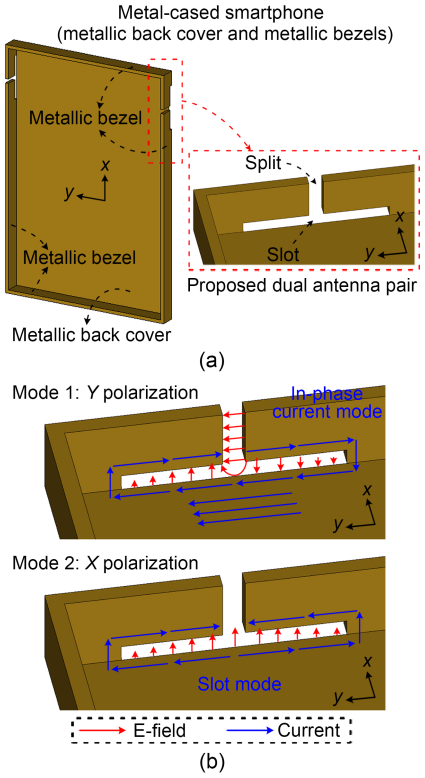

Fig. 1 The metal-cased phone model (a) and the operating modes of the proposed dual antenna pair (b)

If the two modes can be excited properly, a dual antenna pair with high independence can be obtained. This novel antenna pair without ground clearance is suitable for use in metal-cased smartphones.

3 Dual antenna pair

Fig. 2a shows the structure of the proposed dual antenna pair. Several 0.8-mm-thick FR-4 substrates

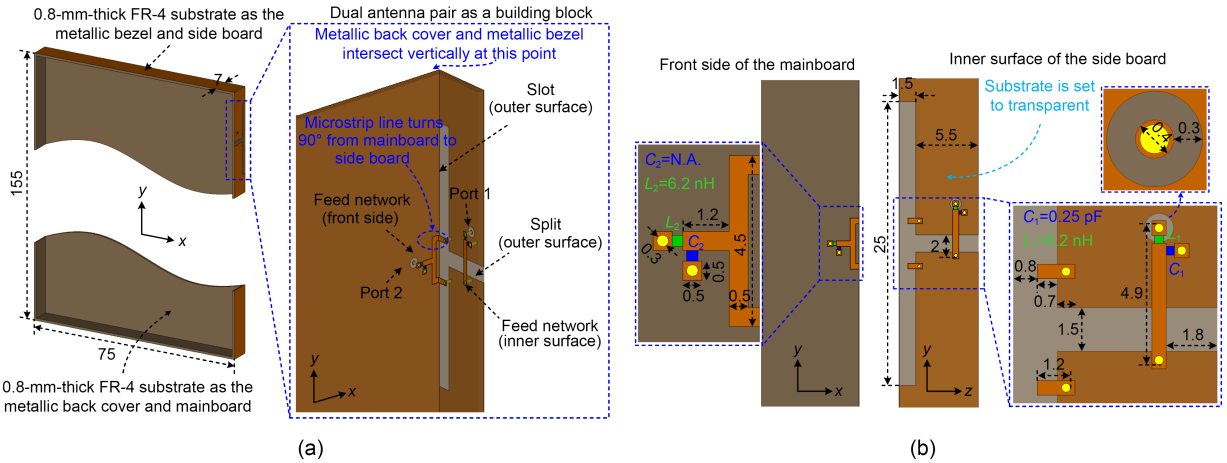

Fig. 2 The structure of the proposed dual antenna pair (a) and the dimensions of the realized sub-6-GHz dual antenna pair (b) (unit: mm). References to color refer to the online version of this figure

(ε_r=4.4, tan δ=0.02) were used to imitate the metallic back cover and four metallic bezels. For the main board in the *XY* plane, a whole metal pattern on the back side acted as the complete metallic back cover and no ground clearance needed to be reserved. For the side boards in the *YZ* and *XZ* planes, the whole metal patterns on the outer surfaces acted as the metallic bezels. The metallic back cover connected with the four metallic bezels vertically at the bottom opening of the cavity formed by the four bezels, constituting the system ground. The dimension of the main board was 155 mm×75 mm; and the height of the side board was 7 mm; these sizes are common for a modern smartphone.

The zoom-in view of the proposed antenna pair is shown in the blue dashed rectangle. A symmetrical T-shaped slot was etched off from the right bezel. Two feeding networks located on the front side of the main board and on the inner surface of the side board were used to excite the two characteristic modes. Ant1, the in-phase current antenna, was excited using the odd mode excitation method, which means that a 180° potential difference was built across the split. A microstrip line that passes the split with property was used to excite this mode. Ant2, the slot antenna, was excited using the even mode excitation method, which indicated that the two sides of the split are equipotential. A symmetrical Y-shaped end-shorted network was used to excite the slot mode. Note that the Y-shaped network moved from the main plate to the side plate with a 90° turnaround. The ideal symmetry of Ant2, including the symmetrical Y-shaped network and T-shaped slot, was important for guaranteeing high port isolation. For both antennas, two lump components (inductor and capacitor) were adopted for antenna matching (Li Y et al., 2010a).

The detailed dimensions of the sub-6-GHz dual antenna pair are illustrated in Fig. 2b, which shows the front side of the main board and the inner surface of the side board (the substrate was set to transparent). The proposed dual antenna pair was simulated using the computer simulation technology (CST), version of 2017. The simulation results are shown in Figs. 3 and 4. Note that the parasitic parameters and intrinsic resistors of the lump components have been taken into account in the simulation. As shown in Fig. 3a, the reflection coefficients for Ant1 and Ant2 were better than −10.1 dB and −6.9 dB, respectively. Owing to orthogonal polarization, isolation was better than 24.5 dB across the pass band. The feeding network is the key to ensure orthogonality. For Ant1, a 180° phase difference was established across the split by the microstrip line with the end-shorted property, so all the symmetrical points on the two open slots had the out-of-phase property. For Ant2, a Y-shaped network was used to feed the T-shaped structure, so all the symmetrical points on the two open slots had the same phase due to the symmetry structure. As a result, the energy from port 1 cannot flow to port 2, and vice versa, achieving high isolation. Fig. 3b shows the ECC. The simulated ECC was lower than 0.01 in the −6 dB operation band, indicating that the

proposed antenna pair had little correlation. On the other hand, antenna irrelevance can be observed intuitively from radiation patterns. The radiated direction of the proposed antenna pair was nearly orthogonal, which is contributed mainly by the orthogonal polarization property. Ant1's main lobe pointed in the $-Y$ direction, whereas Ant2's main lobe pointed in the $-X$ direction. Good isolation and irrelevance levels indicated that the two antennas have good diversity performance. Fig. 3c shows the total efficiencies of the two antennas: 50.3%–55.2% for Ant1 and 50.1%–63.1% for Ant2. Fig. 4 shows the vector E-field and current distributions on the antenna aperture, and the ground current distributions at 3.5 GHz. The field distributions were consistent with the two modes analyzed in Fig. 1. When port 1 was excited, a strong E-field was constructed across the split, and two quarter waves with 180° phase difference were observed around the slot. An in-phase current distributed around the slot and longitudinal ground (Y-directed) current was excited. When port 2 was excited, the classic slot mode was observed and there was no potential difference across the split. Because the currents along the longitudinal direction flowed in opposite directions, transverse direction (X-directed) ground current was excited.

4 Fabricated four-antenna MIMO system

To verify the feasibility, a four-antenna MIMO system was fabricated and tested, consisting of block 1 and block 2. Fig. 5 shows the fabricated prototype. For Ant1 and Ant3, a 10 nH shunt coil inductor cascaded by a 0.3 pF capacitor in series with a 0.2 pF capacitor was adopted for impedance matching. For Ant2 and Ant4, only one 6.8 nH series coil inductor was adopted.

Fig. 6 shows the simulation and measurement results of the four-antenna system. The simulation and measurement results agreed well, and the slight discrepancies came from hand-made errors and differences in the parasitic parameters of lump components between simulation and measurement. In measurement, when

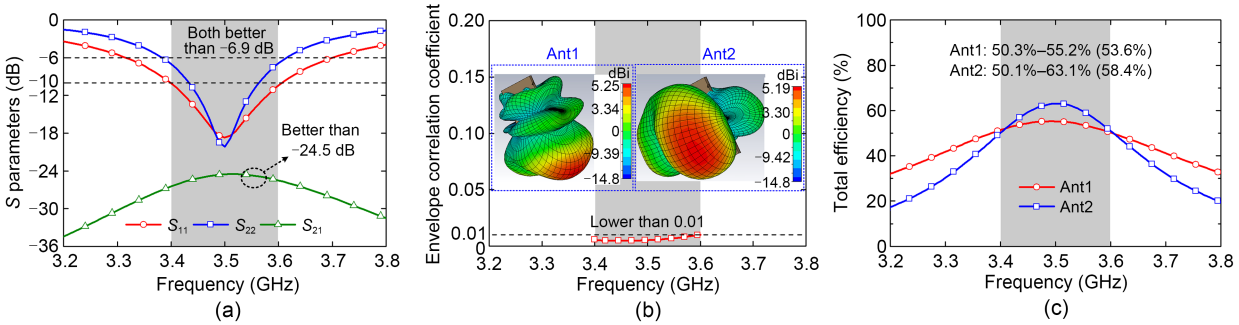

Fig. 3 Simulation results of the proposed dual antenna pair: (a) *S* parameters; (b) ECC (realized gain patterns at 3.5 GHz are shown in the insets); (c) total efficiency

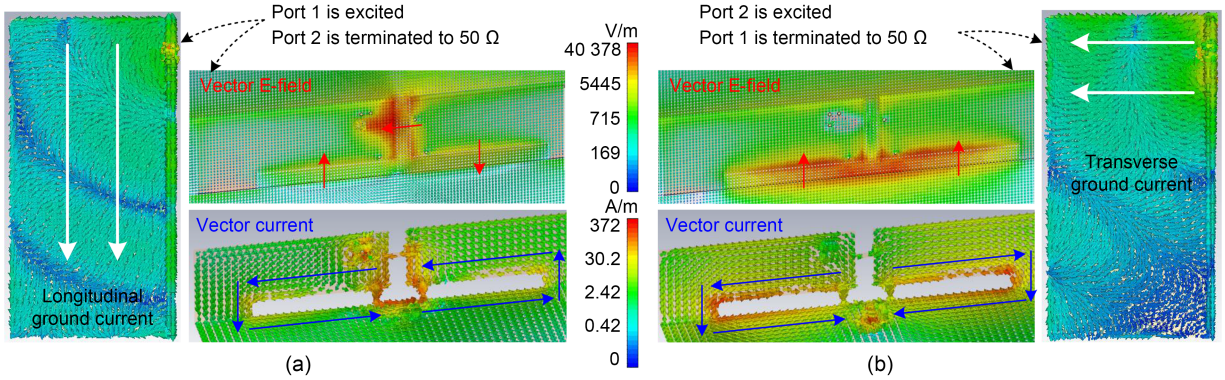

Fig. 4 Field distributions on antenna aperture and ground current distributions at 3.5 GHz: (a) in-phase current antenna; (b) slot antenna

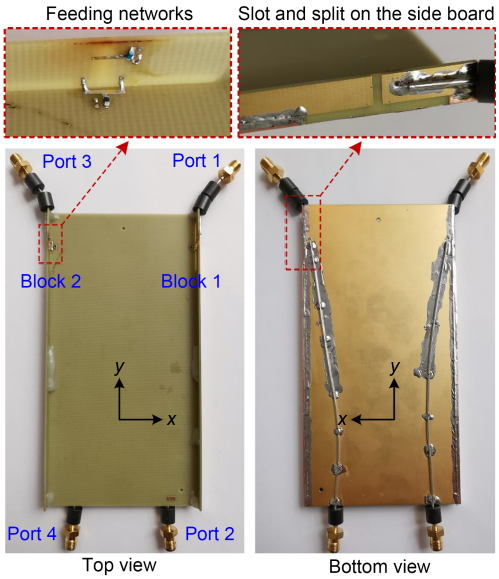

Fig. 5 Fabricated prototype of the four-antenna MIMO system

one or two ports were excited, the remaining non-active ports were terminated to 50 Ω matching loads. The measured reflection coefficients and isolations satisfied the −6 dB and −10 dB criteria, respectively. In simulation, the worst measured isolation occurred between the two slot antennas, Ant2 and Ant4, but the isolation of S_{42} was still lower than −15.0 dB. For the proposed dual antenna pair, the measured isolations were better than −16.9 dB for block 1 and −18.1 dB for block 2. Measured isolations of any other two antennas were better than −27.9 dB. The measured total efficiency ranges were 43.5%–56.8% for Ant1, 40.5%–47.6% for Ant2, 43.6%–61.9% for Ant3, and 43.1%–53.5% for Ant4. The measured ECCs of both antennas were lower than 0.13, so the four antennas showed little correlation. Measurement results demonstrated the feasibility of the proposed scheme for the realization of the dual antenna pair.

5 Conclusions

A dual antenna pair with orthogonal polarization and zero ground clearance property suitable for metal-cased 5G MIMO smartphone was proposed. Two orthogonal degenerate characteristic modes, including the in-phase current and slot modes, were excited on the single antenna structure. A four-antenna MIMO system was fabricated, and the measurement results demonstrated the feasibility of the device.

Contributors

Le CHANG conceived the idea and supervised the project, in consultation with Juan CHEN. Wenbao HE and Xiaomin CHEN carried out the full-wave simulations and partially launched the experiments. Xiaoxue TAN, Kai KANG, and Yang YANG assisted in assembling the tested prototypes and constructed the experiment setup. All authors discussed the theoretical and numerical aspects, and interpreted the results. Le CHANG drafted the paper. All authors revised and finalized the paper.

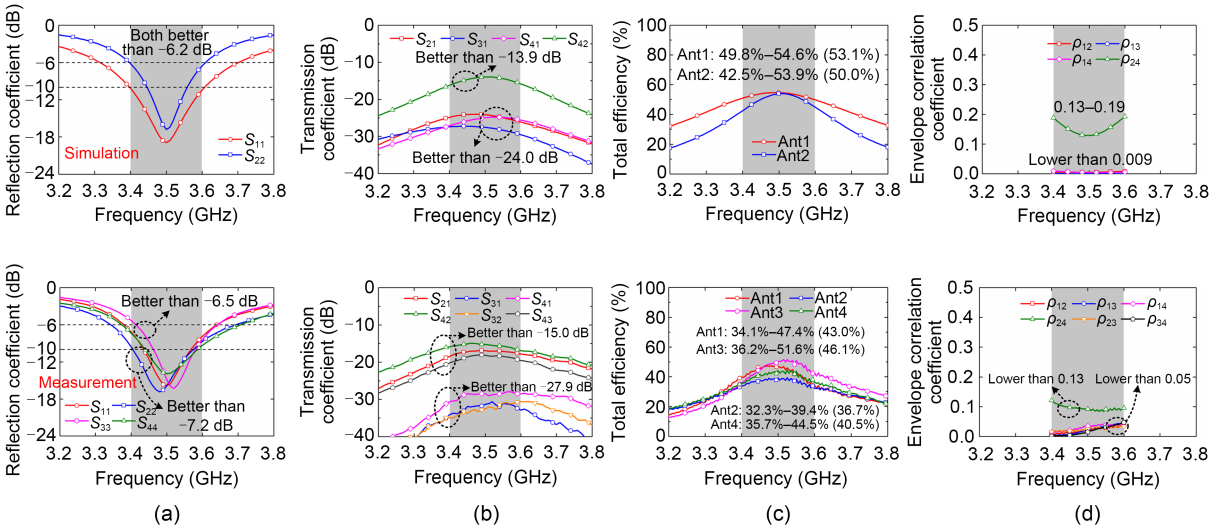

Fig. 6 Simulation and measurement results of the four-antenna MIMO system: (a) reflection coefficient; (b) isolation; (c) total efficiency; (d) ECC (The first row shows the simulation and the second shows the measurement)

Compliance with ethics guidelines

Le CHANG, Wenbao HE, Xiaomin CHEN, Xiaoxue TAN, Juan CHEN, Kai KANG, and Yang YANG declare that they have no conflict of interest.

References

Chang L, Yu YF, Wei KP, et al., 2019. Polarization-orthogonal co-frequency dual antenna pair suitable for 5G MIMO smartphone with metallic bezels. *IEEE Trans Antenn Propag*, 67(8):5212-5220. https://doi.org/10.1109/TAP.2019.2913738

Chang L, Yu YF, Wei KP, et al., 2020. Orthogonally polarized dual antenna pair with high isolation and balanced high performance for 5G MIMO smartphone. *IEEE Trans Antenn Propag*, 68(5):3487-3495. https://doi.org/10.1109/TAP.2020.2963918

Chang L, Zhang GL, Wang HY, 2021. Dual-band antenna pair with lumped filters for 5G MIMO terminals. *IEEE Trans Antenn Propag*, 69(9):5413-5423. https://doi.org/10.1109/TAP.2021.3060827

Chen QG, Lin HW, Wang JP, et al., 2019. Single ring slot-based antennas for metal-rimmed 4G/5G smartphones. *IEEE Trans Antenn Propag*, 67(3):1476-1487. https://doi.org/10.1109/TAP.2018.2883686

Deng CZ, Xu Z, Ren AD, et al., 2019. TCM-based bezel antenna design with small ground clearance for mobile terminals. *IEEE Trans Antenn Propag*, 67(2):745-754. https://doi.org/10.1109/TAP.2018.2880045

Han CZ, Liao SM, Hong KD, et al., 2019. A frequency-reconfigurable antenna with 1-mm nonground portion for metal-frame and full-display screen handset applications using mode control method. *IEEE Access*, 7:48037-48045. https://doi.org/10.1109/ACCESS.2019.2909172

Hong W, 2017. Solving the 5G mobile antenna puzzle: assessing future directions for the 5G mobile antenna paradigm shift. *IEEE Microw Mag*, 18(7):86-102. https://doi.org/10.1109/MMM.2017.2740538

Huang DW, Du ZW, Wang Y, 2019. Eight-band antenna for full-screen metal frame LTE mobile phones. *IEEE Trans Antenn Propag*, 67(3):1527-1534. https://doi.org/10.1109/TAP.2018.2888805

Li MY, Xu ZQ, Ban YL, et al., 2017a. Eight-port orthogonally dual-polarised MIMO antennas using loop structures for 5G smartphone. *IET Microw Antenn Propag*, 11(12):1810-1816. https://doi.org/10.1049/iet-map.2017.0230

Li MY, Ban YL, Xu ZQ, et al., 2017b. Tri-polarized 12-antenna MIMO array for future 5G smartphone applications. *IEEE Access*, 6:6160-6170. https://doi.org/10.1109/ACCESS.2017.2781705

Li Y, Zhang ZJ, Chen WH, et al., 2009. A quadband antenna with reconfigurable feedings. *IEEE Antenn Wirel Propag Lett*, 8:1069-1071. https://doi.org/10.1109/LAWP.2009.2031415

Li Y, Zhang ZJ, Chen WH, et al., 2010a. A dual-polarization slot antenna using a compact CPW feeding structure. *IEEE Antenn Wirel Propag Lett*, 9:191-194. https://doi.org/10.1109/LAWP.2010.2044865

Li Y, Zhang ZJ, Chen WH, et al., 2010b. A switchable matching circuit for compact wideband antenna designs. *IEEE Trans Antenn Propag*, 58:3450-3457. https://doi.org/10.1109/TAP.2010.2071345

Li Y, Zhang ZJ, Feng ZH, et al., 2011. Dual-mode loop antenna with compact feed for polarization diversity. *IEEE Antenn Wirel Propag Lett*, 10:95-98. https://doi.org/10.1109/LAWP.2011.2112752

Li Y, Zhang ZJ, Zheng JF, et al., 2012. A compact hepta-band loop-inverted F reconfigurable antenna for mobile phone. *IEEE Trans Antenn Propag*, 60(1):389-392. https://doi.org/10.1109/TAP.2011.2167949

Sharawi MS, Ikram M, Shamim A, 2017. A two concentric slot loop based connected array MIMO antenna system for 4G/5G terminals. *IEEE Trans Antenn Propag*, 65(12): 6679-6686. https://doi.org/10.1109/TAP.2017.2671028

Sun LB, Feng HG, Li Y, et al., 2018. Compact 5G MIMO mobile phone antennas with tightly arranged orthogonal-mode pairs. *IEEE Trans Antenn Propag*, 66(11):6364-6369. https://doi.org/10.1109/TAP.2018.2864674

Wong KL, Tsai CY, 2016. IFA-based metal-frame antenna without ground clearance for the LTE/WWAN operation in the metal-casing tablet computer. *IEEE Trans Antenn Propag*, 64(1):53-60. https://doi.org/10.1109/TAP.2015.2503420

Wong KL, Tsai CY, 2017. Half-loop frame antenna for the LTE metal-casing tablet device. *IEEE Trans Antenn Propag*, 65(1):71-81. https://doi.org/10.1109/TAP.2016.2630716

Wong KL, Tsai CY, Li WY, 2017a. Integrated yet decoupled dual antennas with inherent decoupling structures for 2.4/5.2/5.8-GHz WLAN MIMO operation in the smartphone. *Microw Opt Technol Lett*, 59(9):2235-2241. https://doi.org/10.1002/mop.30717

Wong KL, Lin BW, Li BWY, 2017b. Dual-band dual inverted-F/loop antennas as a compact decoupled building block for forming eight 3.5/5.8-GHz MIMO antennas in the future smartphone. *Microw Opt Technol Lett*, 59(11):2715-2721. https://doi.org/10.1002/mop.30811

Wong KL, Tsai CY, Lu JY, 2017c. Two asymmetrically mirrored gap-coupled loop antennas as a compact building block for eight-antenna MIMO array in the future smartphone. *IEEE Trans Antenn Propag*, 65(4):1765-1778. https://doi.org/10.1109/TAP.2017.2670534